30th Annual International IEEE EMBS Conference
Vancouver, British Columbia, Canada, August 20-24, 2008

Eigenvector Analysis for Separation of a Spectrally Concentrated Source from a Mixture

Ronald Phlypo, Vicente Zarzoso and Ignace Lemahieu

Abstract— **An objective function is presented to recover a spectrally narrow band signal from multichannel measurements, as in electrocardiogram recordings of atrial fibrillation. The criterion can be efficiently maximized through the eigenvalue decomposition of some spectral correlation matrices of the whitened observations across appropriately chosen frequency bands. It is conjectured that the global optimum so attained recovers the source of interest when its spectral concentration around its modal frequency is maximal. Numerical experiments on synthetic data seem to support the validity of this hypothesis. Moreover, the components extracted from a patient data set with known atrial fibrillation show the characteristics of the associated f-wave as described in medical literature.**

I. INTRODUCTION

Atrial Fibrillation (AF) and atrial flutter (AFL) are the most prevalent cardiac arrhythmia encountered in clinical practice and accounts for approximately one third of the hospital admissions for cardiac rhythm disturbances. Its prevalence is about 0.4-1.0% in the general population and increases with age to reach up to 9% of the population aged 80 years and older. Amongst others, because of an aging population and more frequent monitoring, during the past 20 years there has been an increase of hospitalization of about 66%. This trouble is also associated with an augmented risk of stroke, heart failure and all-cause mortality [1].

Diagnostization and characterization of AF/AFL is mainly based on the noninvasive electrocardiographic (ECG) signals and has evolved from simple f-wave amplitude characterization to the estimation of spectral parameters [2]. However, the ventricular waveforms (QRS-T) have an amplitude many times larger than the atrial wave to be characterized and thus masks our signal of interest, as can be seen in Figure 1.

Proposed techniques to solve for this masking are based on the cancellation of the ventricular contribution in the ECG [3] or the decomposition into independent components (ICA) [4], whether or not with some priors on the signal of interest or its nullspace [5], [6]. Despite their popularity they suffer from some major drawbacks. The cancellation methods require a robust R-wave detection to synchronize the waveforms. Moreover, they neither make use of the spatial interdependencies of the leads, except for a possible rotation of the main electrical axis of the heart, neither do they account for individual waveform variations of the complexes. On the contrary, the spatial ICA based methods do take into account the spatial dependencies of the signals and are not affected by individual waveform variations, but they are generally not well suited for sources whose distribution parameters (higher order cumulants) are close to those of a Gaussian, unless its sub-Gaussian character is taken into account [5] or additional temporal information is used [6].

This work was supported by FWO contract number G.0095.05

R. Phlypo and I. Lemahieu are with Ghent University - IBBT, IbiTech-MEDISIP, Ghent, Belgium {ronald.phlypo, ignace.lemahieu}@ugent.be

V. Zarzoso is with I3S, University of Nice-Sophia Antipolis - CNRS, Sophia Antipolis, France zarzoso@i3s.unice.fr

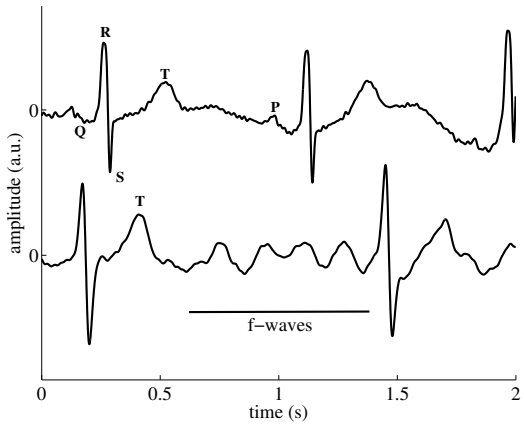

Fig. 1. Example of normal sinus rhythm (upper) and atrial fibrillation wave (lower)

However, the method of [5] deals only with the separation of two observations into two signals in its original version, namely the ventricular, respectively the atrial signal. The method of [6] makes use of an empirical parameter to threshold the cumulants of the signals obtained by ICA. The signals having cumulants below the threshold are subsequently fed to a spatiotemporal decorrelation method. However, the kurtosis threshold is chosen empirically, and the method is bound to provide poor results when the atrial activity cannot be fully separated from the ventricular activity by the initial ICA stage. All of the above methods are based on numerical optimization and even if some of them are feasible under multiple iterations of partial closed-form solutions, they all lack a final solution that can be represented as a global optimum for a well-defined function for AA estimation.

This contribution proposes the spectral concentration indicator of [6] as an explicit criterion for the extraction of an estimate of the AF/AFL source, and shows that it can be cost-effectively maximized by the eigenvalue decomposition of some well-chosen spectral correlation matrices of the available data.

II. METHODS

A. Notation

Scalars, constants, column vectors and matrices are represented by thin face lower case, light face upper case, bold

face lower case and bold face upper case, respectively. The Fourier transform of a time series $x[n]$ is represented by $\tilde{x}(\omega)$.

B. Data and Preprocessing

We use 30 patient datafiles recorded at the Clinical University Hospital, Valencia, Spain, using a Prucka Eng. Cardiolab system with 12-leads, sampled at $f_s = 1000$ time samples per second [6]. All patients were under treatment of amiodarone. Baseline wander has been canceled out by a zero-phase 12^{th} order Chebychev filter with minimum passband ripple.

The simulated dataset is made up of 3 basis waveforms ($\mathbf{s}[n]$), namely a triangular waveform ($s_1[n]$), an impulsive waveform ($s_2[n]$) and stochastic non-Gaussian noise ($s_3[n]$) to simulate respectively AF/AFL, a QRS-wave complex and noise[1].

C. Linear Spatial Filtering

Consider N time samples taken from a 12-lead ECG, $\mathbf{y}[n] \in \mathbb{R}^{12}, n = 1 \dots N$ and a spatial mixing channel $\mathbf{a} \in \mathbb{R}^{12}$, such that $\mathbf{y}[n] = \mathbf{a}s[n] + \eta[n]$, where $s[n] \in \mathbb{R}$ is the atrial (fibrillatory or flutter) activity and $\eta \in \mathbb{R}^{12}$ is the activity in the recording $\mathbf{y}[n]$ that is not related to the atrial activity. This model can be seen as a first order approximation of a spatially fixed collection of oriented dipoles whose activity is measured at the body surface, assuming that the body tissues behave as a purely resistive propagation medium in the frequency range of interest [7]. From the measurement setup, it can easily be seen that η accounts for external noise and other physiological electrical source contributions, amongst others the ventricular activity.

Our goal is to inverse the above system by finding the linear filter $\mathbf{w}$ that recovers an estimate of the auricular activity $\hat{x}[n] = \mathbf{w}^T\mathbf{y}[n]$ at its output.

D. An objective function for AF/AFL

Consider now the spectral concentration (SC) indicator [6], given as:

$$\mathrm{SC}(x) = \frac{1}{\mathbf{P}_x} \int_{0.872 f_m}^{1.125 f_m} |\tilde{x}(f)|^2 \mathrm{d}f \qquad (1)$$

where $|\cdot|$ denotes the absolute value of $\tilde{x}(f)$, f_m is the modal frequency and $\mathbf{P}_x$ is the total power of x, i.e. $\int_0^N |x[n]|^2 \mathrm{d}n$. Now, under the assumption that our AF/AFL signal is narrow band around the modal frequency f_m and $\tilde{x}$ has maximum power in the frequency band $[0.875 f_m, 1.125 f_m]$Hz with respect to any other linear combination of η and s, (1) has a maximum for AF/AFL. Furthermore, the optimum is available under a closed form expression of eigenvalues, hence we call the method described next Eigenvalue-based Spectral Optimization (ESO).

Remark that since in this work $x[n] \in \mathbb{R}$, we have $\tilde{x}(f_1)\tilde{x}^\star(f_1) = \tilde{x}(f_s - f_1)\tilde{x}^\star(f_s - f_1) = |x(f_1)|^2$, where $\tilde{x}^\star$ is the complex conjugate of $\tilde{x}$. We can thus use uniquely positive frequency values without changing the value of (1).

[1]Matlab files containing the generators and the algorithm can be downloaded from http://users.ugent.be/∼rphlypo/software/

E. Prewhitening

Maximizing (1) can be done by maximizing the nominator under a constant denominator constraint. Therefore, we will subdivide our problem into two subproblems, as $s[n] = \mathbf{w}^T\mathbf{y}[n] = \mathbf{q}^T\mathbf{V}^T\mathbf{y}[n]$, where $\mathbf{q} \in \mathbb{R}^m$ and $\|\mathbf{q}\|_2 = 1$. The matrix $\mathbf{V} \in \mathbb{R}^{m \times m}$ is a matrix which will guarantee that the denominator in (1) will remain constant under unit norm projections. Denote by $\mathbf{z}[n]$ the transformed variables $\mathbf{V}^T\mathbf{y}[n]$, with $\mathcal{E}\{\mathbf{z}^T\mathbf{z}\} = \mathbf{I}_m$, where $\mathcal{E}\{\cdot\}$ is the expectation value and $\mathbf{I}_m$ the unit matrix in $\mathbb{R}^{m \times m}$. The expectation matrix can be reduced to the identity matrix by taking the columns of $\mathbf{V}$ as $\mathbf{e}_i/\sqrt{\lambda_i}$, where $\mathbf{e}_i$ is the eigenvector associated to the eigenvalue λ_i of the expectation matrix $\mathcal{E}\{\mathbf{y}\mathbf{y}^T\}$. For unit vectors $\mathbf{q}$, we then have

$$\mathbf{P}_x = \mathbf{q}^T \Phi_{\mathbf{z}}^{(0, f_s)} \mathbf{q} = 1 \ , \qquad (2)$$

where $\Phi_{\mathbf{z}}^{(f_1, f_2)} = \mathrm{Re}\left\{\int_{f_1}^{f_2} \tilde{\mathbf{z}}(f)\tilde{\mathbf{z}}^H(f)\mathrm{d}f\right\}$, where $\mathrm{Re}\{\cdot\}$ is the real part of its argument and $(\cdot)^H$ is the Hermitian transpose operator. The identity in (2) can directly be derived from Parseval's identity, $\mathcal{E}\{\tilde{\mathbf{z}}\tilde{\mathbf{z}}^T\} = \mathcal{E}\{\mathbf{z}\mathbf{z}^T\}$.

F. Spectral Optimization under Prewhitening

The only unknown that remains in the system is the vector $\mathbf{q}$. The vector $\mathbf{q}$ that is the solution to our problem is the one which maximizes the nominator in (1), i.e. the quadratic equation

$$\Psi(x) = \Psi\mathbf{q} = \mathbf{q}^T \Phi_{\mathbf{z}}^{(0.875 f_m, 1.125 f_m)} \mathbf{q} \ . \qquad (3)$$

The maximum of equation (3) can be found by looking for the eigenvector associated to the largest eigenvalue of (3). However, solving for the eigenvector requires the knowledge of the modal angular frequency f_m. In what follows we show that the modal frequency can be estimated by solving two maximum eigenvalue subproblems.

G. Estimation of $\hat{f}_m$

The modal frequency is not known *a priori* and should be estimated from the set of observations. We will rely here on the prior knowledge that the frequency of AF/AFL generally lies in the interval 3-9Hz [1]. However, as can be seen from Figure 2, this is also the frequency interval on which the T-wave has its major power contribution. We thus need to be able to distinguish between both activities. To this extent we make use of the fact that notwithstanding their spectral overlap, they do not share the same spectral parameters. Figure 2 shows that the AF/AFL spectrum is much more concentrated around the modal angular frequency than is the T-wave spectrum and that its modal frequency differs, and this is usually the case.

To separate the two activities, we propose to extract two intermediate components $\hat{x}_1$ and $\hat{x}_2$ by applying the filters according to the eigenvectors that are associated to the largest eigenvalues of the spectral matrices $\Phi_{\mathbf{z}}^{(3,6)}$, respectively $\Phi_{\mathbf{z}}^{(5,9)}$. For the two resulting estimates, $\hat{x}_1$ and $\hat{x}_2$, we estimate their respective modal frequency $\hat{f}_m^{x_1}$ and $\hat{f}_m^{x_2}$, together with their spectral concentration in the spectral band

TABLE I

THE PERCENTILES OF THE SPECTRAL CONCENTRATION DIFFERENCES BETWEEN $x_1[n]$ AND $s_1[n]$

percentile	0	1	25	50	75	99	100
ESO (%)	-4.93	-0.18	0.01	0.03	0.08	0.48	1.31
ST-BSS (%)	-26.20	-1.93	-0.27	-0.07	-0.01	0.20	2.10
ESO w.r.t. ST-BSS (%)	-4.84	-0.22	0.04	0.10	0.33	2.21	26.18

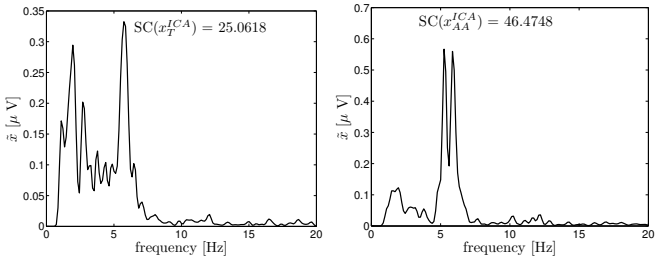

Fig. 2. Example of the power spectral density for the T-wave component (left) and atrial fibrillation (right) as estimated by the COM2 ICA algorithm [8] with SC (1) around $\hat{f}_m = \arg\max_f \tilde{x}(f)$ [in %].

as defined in (1). Finally, we use the estimate $\hat{f}_m = \hat{f}_m^{x_i}$, where i is associated with the intermediate component who has the highest spectral concentration. We then optimize for the spectral concentration around $\hat{f}_m$ as described above (section II-F).

III. RESULTS

A. Simulated Data

We will first show results on a simulated dataset, since it allows to compare the algorithm objectively with existing algorithms. The results over 1000 Monte Carlo realisations have been taken to extract $x_1[n]$ from the observations ($\mathbf{y}[n]$) generated through a full rank mixing ($\mathbf{A}$) of the above three sources $\mathbf{s}[n]$. The parameters of the algorithm have been set to look for the modal frequency in the 1-20 Hz frequency band prior to optimizing the spectral concentration. We compare it to a spatio-temporal blind source separation method ST-BSS [6] where the time delay vector for joint diagonalization has been adapted to include, next to 0 and 1, all prime numbers in the interval $[0, 100]$. This guarantees a lower susceptibility to the prior on the frequency band and is valid in the simulation case since we know from the set-up that there is only a single narrow banded source.

Results for the spectral concentration with respect to its value for the simulated waveform $s_1[n]$ are given in Table I for both the proposed method (ESO) and ST-BSS. The modal frequency has been estimated correctly in both cases with a mean value of zero and no significant outliers (p-value is 1 for a Wilcoxon rank sum test against a Dirac Delta distribution at zero with no rejection of the null-hypothesis at a 10^{-6} confidence level). The mean and standard deviation of the correlation coefficients between $x_1[n]$ and $s_1[n]$ amount to 0.9994 ± 0.0010 for ESO, respectively 0.9991 ± 0.0011 for ST-BSS (minima 0.9928 and 0.9933, maxima 1.0000 and 1.0000, respectively).

B. Patient Data

To evaluate the algorithm's performance we calculate the spectral concentration and estimate the modal frequency of the estimate obtained by the presented method optimized around $\hat{\omega}_m$ (ESO), respectively in the full 3-9Hz frequency band (ESO-fb), ST-BSS [6] (with the time delays as chosen in the original paper) and a maximum likelihood based blind source separation algorithm (ML-BSS) [5].

TABLE II

SC (1) AND $\hat{f}_m = \hat{\omega}_m f_s$ FOR THE SOURCE SIGNALS ESTIMATED WITH ESO AND TWO BSS METHODS ($\mu \pm \sigma$).

	SC	$\hat{f}_m$
ESO	51.11±17.25	5.31±1.22
ESO-fb	40.82±18.55	5.72±1.08
ST-BSS	42.21±17.15	5.13±1.39
ML-BSS	13.66±6.37	5.06±1.44

The results for the spectral concentration and the modal frequency estimate are given in table II as their mean and standard deviation obtained from the dataset.

Since the above results are unable to show the relation between the parameters calculated on the estimates by the different methods on the same data, we give the differences of the spectral concentration and modal frequency between the source $x[n]$ estimated by ESO and $x[n]$ as estimated by the methods ESO-fb, ST-BSS and ML-BSS, respectively, in Figure 3.

The correlation of the parameters over the methods is only obvious for ESO and ST-BSS ($\rho_{SC} = 0.88$ and $\rho_{\hat{\omega}_m} = 0.85$), while the ESO-fb method correlates only slightly with ESO and ST-BSS for the spectral concentration ($\rho_{SC} = 0.52$ in both cases), whilst the modal frequency correlation is $\rho_{\hat{\omega}_m} = 0.14$ with respect to both methods (and even negatively with respect to ML-BSS). The parameters of ML-BSS have no correlation that is beyond 0.25 for both spectral concentration values and modal angular frequencies.

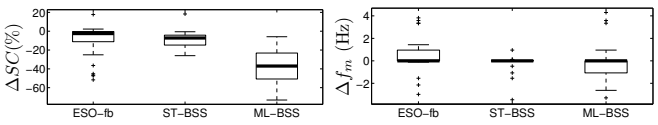

Fig. 3. Box-Whiskers plots of the differences between the parameters of the estimated sources with respect to the ESO method.

In Figure 4 we show a detail of an original data record and the estimated sources by ESO, ST-BSS and ML-BSS. The plots are given for illustrative purposes and show that the solution is physiologically interpretable and in line with medical expectations, namely a sawtooth wave with a modal frequency in the 4-9Hz band [1].

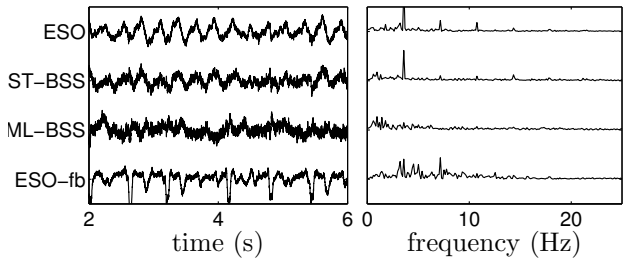

Fig. 4. Example of the AA source estimates on real data: (left) zoom on the V1-lead potentials and the estimated time courses with (right) the absolute values of their respective Fourier terms obtained by a FFT (all signals have arbitrary units).

IV. DISCUSSION

The results obtained from the simulations show that the presented method is able to extract a waveform with the same modal frequency and similar spectral concentration as the original waveform $s_1[n]$. Differences are noticeable through small changes in the spectral concentration value, because our model assumes total orthogonality between $s_1[n]$ and the other contributions $\eta[n]$. This orthogonality was not a prerequisite in the simulation set up and thus some source information might be wrongly estimated due to the mismatch of the simulations with our assumed model. However, as one can see from section III-A, the estimation is fairly close to the original source when considering the correlation coefficient.

Results on real data show that the frequencies estimated by the algorithm are in line with the results obtained by [6] and with clinical knowledge [1]. From Figure 3, it can be observed that the spectral concentration is greater almost everywhere when calculated from the ESO estimate than for the other two algorithms or the estimate in the whole 4-9Hz band. This result may not be surprising, since our algorithm optimizes explicitly for the spectral concentration.

Accordingly to this direct maximization of the spectral concentration for the ESO estimate, we observe that for the example given in Figure 4 the spectral noise floor is lowered and the multi-modality, or harmonic structure of the waveform, becomes more articulated. The former is a property that follows directly from the definition of our function (1) under a constant denominator, while the latter is connected to the application of a spatial filter. Since we optimize for the variance in the narrow band around the estimated frequency $\hat{f}_m$, the constant variance constraint assures that the variance outside this spectral band is kept as low as possible, which explains the lower noise floor. However, the spatial filter $\mathbf{q}$ requires that the estimated signal stems from a fixed spatial origin (not necessarily a single spatial point) and has a fixed orientation [7]. Because a spatial filter makes no distinction in spectral content and acts as a spatial band pass filter for all activity that stems from its physical origin(s), the source of interest with maximum spectral concentration in the band of interest (either 3-6Hz, either 5-9Hz), will be recuperated at the output of the filter $\mathbf{q}$ with its harmonics, even though they penalize SC (1).

In addition, the method is flexible and can easily be extended to optimize for non-stationary spectra, either through direct optimization of the (weighted) sum of the time-varying frequency covariance matrices around $\hat{\omega}_m[k]$ as defined in (1), where k represents the frame index, or through a joint diagonalization of these spectral covariance , along the lines of [9].

V. CONCLUSION

We propose to estimate the atrial activity in ECG recordings of AF by maximizing the spectral concentration of the linear extractor output signal. After prewhitening the multichannel data and estimating the modal frequency $\hat{f}_m$, the optimal spatial filter is found as the dominant eigenvector of the spectral correlation matrix of the whitened observations around that frequency. The global optimum of the criterion can be obtained by computationally efficient eigenvector analysis and, in experiments, is seen to extract the targeted source if it presents maximal spectral concentration around its modal frequency $\hat{f}_m$. The present technique is not limited to the extraction of atrial activity in AF ECGs, but can probably be extended with minor modifications to any problem requiring the estimation of narrowband signals from multichannel measurements, in biomedicine or other fields. Current work aims at determining the conditions under which the proposed criterion is indeed a contrast function for source extraction.

VI. ACKNOWLEDGMENTS

The authors gratefully acknowledge F. Castells and the Electrophysiology Laboratory of the University Clinical Hospital of Valencia, Spain for sharing the data with us.

REFERENCES

[1] ACC/AHA/Physician Consortium 2008, "Clinical performance measure for adults with nonvalvular atrial fibrillation or atrial flutter," *Circulation*, pp. 1100–1120, 2008 doi: 10.1161/CIRCULATIONAHA.107.187192.

[2] M. Stridh, L. Sörnmo, C. Meurling, and B. Olsson, "Sequential characterization of atrial tachyarrhythmias based on ECG time-frequency analysis," *IEEE Trans on Biomed Eng*, vol. 51, pp. 100–114, 2004.

[3] M. Stridh and L. Sörnmo, "Spatiotemporal qrst cancellation techniques for analysis of atrial fibrillation." *IEEE Trans Biomed Eng*, vol. 48, no. 1, pp. 105–111, Jan 2001.

[4] J. J. Rieta, F. Castells, C. Sánchez, V. Zarzoso, and J. Millet, "Atrial activity extraction for atrial fibrillation analysis using blind source separation." *IEEE Trans Biomed Eng*, vol. 51, no. 7, pp. 1176–1186, Jul 2004.

[5] F. Castells, J. Igual, J. Millet, and J. Rieta, "Atrial activity extraction from atrial fibrillation episodes based on maximum likelihood source separation," *Signal Processing*, vol. 85, pp. 523–535, 2005.

[6] F. Castells, J. Rieta, J. Millet, and V. Zarzoso, "Spatiotemporal blind source separation approach to atrial activity estimation in atrial tachyarrhythmias," *IEEE Transactions on Biomedical Engineering*, vol. 52, no. 2, pp. 258–267, Feb. 2005.

[7] J. Malmivuo and R. Plonsey, *Bioelectromagnetism: Principles and Applications of Bioelectric and Biomagnetic Fields*. New York: Oxford University Press, 1995.

[8] P. Comon, "Independent component analysis, a new concept?" *Signal Processing*, vol. 36, pp. 287–314, 1994.

[9] J.-F. Cardoso and A. Souloumiac, "Jacobi angles for simultaneous diagonalization." *SIAM Journ on Matrix Analysis and Applications*, vol. 17, no. 1, pp. 161–164, 1996.